

MEaSURES Multi-year Reference Velocity Maps of the Antarctic Ice Sheet, Version 1

USER GUIDE

How to Cite These Data

As a condition of using these data, you must include a citation:

Rignot, E., B. Scheuckl, J. Mouginot, and S. Jeong. 2022. *MEaSURES Multi-year Reference Velocity Maps of the Antarctic Ice Sheet, Version 1*. [Indicate subset used]. Boulder, Colorado USA. NASA National Snow and Ice Data Center Distributed Active Archive Center.
<https://doi.org/10.5067/FB851ZIZYX5O>. [Date Accessed].

FOR QUESTIONS ABOUT THESE DATA, CONTACT NSIDC@NSIDC.ORG

FOR CURRENT INFORMATION, VISIT <https://nsidc.org/data/NSIDC-0761>

TABLE OF CONTENTS

| | | |
|-------|---|----|
| 1 | DATA DESCRIPTION..... | 3 |
| 1.1 | Parameters | 3 |
| 1.2 | File Information | 3 |
| 1.2.1 | Format | 3 |
| 1.2.2 | File Contents | 3 |
| 1.2.3 | Naming Convention | 4 |
| 1.3 | Spatial Information | 4 |
| 1.3.1 | Coverage | 4 |
| 1.3.2 | Resolution..... | 4 |
| 1.3.3 | Geolocation | 5 |
| 1.4 | Temporal Information..... | 5 |
| 1.4.1 | Coverage | 5 |
| 1.4.2 | Resolution..... | 5 |
| 2 | DATA ACQUISITION AND PROCESSING | 6 |
| 2.1 | Acquisition | 6 |
| 2.2 | Processing | 6 |
| 2.3 | Quality, Errors, and Limitations | 6 |
| 3 | VERSION HISTORY | 9 |
| 4 | RELATED DATA SETS | 9 |
| 5 | RELATED WEBSITES..... | 9 |
| 6 | ACKNOWLEDGMENTS | 9 |
| 7 | REFERENCES | 10 |
| 8 | DOCUMENT INFORMATION..... | 11 |
| 8.1 | Publication Date..... | 11 |
| 8.2 | Date Last Updated | 11 |
| | APPENDIX A – SPATIAL AND TEMPORAL COVERAGE BY SATELLITE | 12 |

1 DATA DESCRIPTION

This data set, part of the NASA Making Earth System Data Records for Use in Research Environments (MEaSURES) Program, contains four as-complete-as-possible 450 m resolution reference maps of ice component velocities (v_x , v_y) for the Antarctic ice sheet. Maps are available for 1995 – 2001; 2007 – 2009; 2014 – 2017; and 2020 – 2022.

Component velocities are derived by applying phase analysis and speckle tracking to satellite synthetic aperture radar data, and by feature tracking of visible imagery obtained by the Operational Land Imager (OLI) on board Landsat-8.

Data also include component velocity standard deviation and standard error (mean velocity); the number of observation pairs used for each pixel; start and end dates of input data for each pixel; and a mask that indicates ice front and grounding line locations.

1.1 Parameters

Ice velocity (v_x , v_y)

Standard deviation (v_x , v_y)

Standard error of mean velocity (v_x , v_y)

1.2 File Information

1.2.1 Format

This data set is provided in NetCDF-4 using CF-1.6¹ conventions.

1.2.2 File Contents

Data files contain the variables described in Table 1.

Table 1. Variable Names and Descriptions

| Variable Name | Description | Fill | Data Type |
|---------------------|--|------|-----------|
| CNT | Count of image pairs used in each pixel | N/A | int |
| DATE_SAMPLING_START | Start date (decimal years) of the time coverage for each pixel | 0.0 | float |
| DATE_SAMPLING_END | End date (decimal years) of the time coverage for each pixel | 0.0 | float |

¹ NetCDF Climate and Forecast (CF) Metadata Conventions

| Variable Name | Description | Fill | Data Type |
|---------------|--|------|-----------|
| ERRX | Standard error of mean velocity in the x direction (m/y) | 0.0 | float |
| ERRY | Standard error of mean velocity in the y direction (m/y) | 0.0 | float |
| MASK | 0=ocean; 1=grounded; 2=floating | N/A | byte |
| STDX | Standard deviation of velocity in the x direction (m/y) | 0.0 | float |
| STDY | Standard deviation of velocity in the y direction (m/y) | 0.0 | float |
| VX | Ice velocity in the x direction (m/y) | 0.0 | float |
| VY | Ice velocity in the y direction (m/y) | 0.0 | float |
| crs | Complete description of the coordinate reference | N/A | char |
| lat | Latitude | N/A | double |
| lon | Longitude | N/A | double |
| x | Grid x coordinate (m) | N/A | double |
| y | Grid y coordinate (m) | N/A | double |

1.2.3 Naming Convention

This data set consists of the following data files. The date range for each file is specified in file name:

- antarctica_ice_velocity_1995-2001_450m_v01.1.nc
- antarctica_ice_velocity_2007-2009_450m_v01.1.nc
- antarctica_ice_velocity_2014-2017_450m_v01.1.nc
- antarctica_ice_velocity_2020-2022_450m_v01.1.nc

1.3 Spatial Information

1.3.1 Coverage

South: 90° S

North: 60° S

West: 180° W

East: 180° E

1.3.2 Resolution

450 m × 450 m

1.3.3 Geolocation

Data are provided in the WGS 84/Antarctic Polar Stereographic projection ([EPSG:3031](#)). The following table contains details about the grid.

Table 2. Grid Details

| | |
|--|--------------------------------|
| Grid cell size (x, y pixel dimensions) | 450 m x 450 m |
| Number of rows | 12445 |
| Number of columns | 12445 |
| Location of Origin | Center of grid |
| Geolocated lower left point in grid | 54.67353057861328° S, 225.0° E |
| Grid rotation | N/A |
| ulxmap – x-axis map coordinate of the center of the upper-left pixel (XLLCORNER for ASCII data) | -2,799,775.0 |
| ulymap – y-axis map coordinate of the center of the upper-left pixel (YLLCORNER for ASCII data) | 2,799,775.0 |

1.4 Temporal Information

1.4.1 Coverage

Time periods for each map were chosen to maximize spatial coverage and minimize error compared to annual maps, while still restricting the observation period (for an annual map see [MEaSURES Annual Antarctic Ice Velocity Maps, Version 1](#)):

- 01 July 1995 – 30 June 2001
- 01 July 2007 – 30 June 2009
- 01 July 2014 – 30 June 2017
- 01 July 2020 – 30 June 2022

1.4.2 Resolution

Varies

The spatial and temporal coverage for each satellite and sensor is detailed in “APPENDIX A – SPATIAL AND TEMPORAL COVERAGE BY SATELLITE.”

2 DATA ACQUISITION AND PROCESSING

2.1 Acquisition

The data set was generated from SAR data and visible imagery acquired by the following satellites/sensors:

- ALOS/PALSAR
- ENVISAT/ASAR
- ERS-1/AMI-SAR
- ERS-2/AMI-SAR
- Sentinel-1A/C-SAR
- Sentinel-1B/C-SAR
- RADARSAT-1/SAR
- RADARSAT-2/SAR
- TerraSAR-X/X-SAR
- TanDEM-X/X-SAR
- Landsat-8/OLI

2.2 Processing

Ice velocities were derived using the following interferometric analysis techniques:

- Combining interferometric phases from two independent tracks to retrieve the surface flow vector (Mouginot et al., 2019)
- Augmenting the phase map in coastal areas with speckle tracking in both along-track (azimuth) and across-track (range) directions (Rignot et al., 2011; Mouginot et al., 2012; Mouginot et al., 2017)
- Calculating two-dimensional offsets in amplitude imagery (Mouginot et al., 2012)
- Combining range interferometric phases along two independent tracks (Mouginot et al., 2012)

In all cases, surface parallel flow is assumed. Landsat-8 data were processed using repeat image feature tracking (see Mouginot, et al. 2017).

2.3 Quality, Errors, and Limitations

Data quality is discussed in detail in Rignot, et al. 2011; Mouginot, et al., 2014; and Mouginot, et al. 2017. Ice flow mapping accuracy varies with the sensor, repeat cycle, geographic location, time

period, interferometric analysis technique, and the amount of data stacking. Table 3 lists the range (Rg) and azimuth (Az) error in velocity mapping for each sensor, without data stacking.

Figure 1 shows a plot of ice motion for 1995–2001, 2007–2009, 2014–2017, and 2020–2022, plus standard error in mean speed taking into account errors from the following sources:

- Speckle tracking and interferometric phase analysis (SAR only)
- Ionospheric perturbations, which are strongest in the azimuth direction; stronger in L-band compared to C-band; and stronger in the East Antarctic ice sheet than the West Antarctic ice sheet due to more abundant ionospheric perturbations near the magnetic pole.
- Landsat-8 feature tracking analysis
- Data stacking (reduces error noise as the square root of the number of averaged interferometric pairs)
- Respective instrument weights applied during mosaicking

The total error is computed as the square root of the sum of the independent errors squared. Error estimates in range (Rg) and azimuth (Az) for each sensor, without data stacking, are summarized in Table 3.

Table 3. Error in Ice Velocity Mapping by Sensor

| Platform/Sensor | Nominal Repeat Cycle (days) | Error (m/yr) | |
|-------------------------------------|-----------------------------|-----------------|-----------------|
| | | Rg | Az |
| ALOS (WAIS)/PALSAR | 46 | 6 | 17 |
| ALOS (EAIS)/PALSAR | 46 | 6 | 5 |
| ENVISAT/ASAR | 35 | 21 | 4 |
| RADARSAT-2/SAR | 24 | 26 | 8 |
| RADARSAT-1/SAR | 24 | 26 | 8 |
| Sentinel-1/SAR | 12 | 12 | 43 |
| Landsat-8/OLI | 16 | 34 ² | 34 ² |
| TanDEM-X (TDX)/TerraSAR-X (TSX)/SAR | 11 | 8 | 8 |
| Tandem ERS-1 and -2 (phase)/SAR | 1 | 1 | N/A |

² Landsat uses repeat image feature tracking in x and y

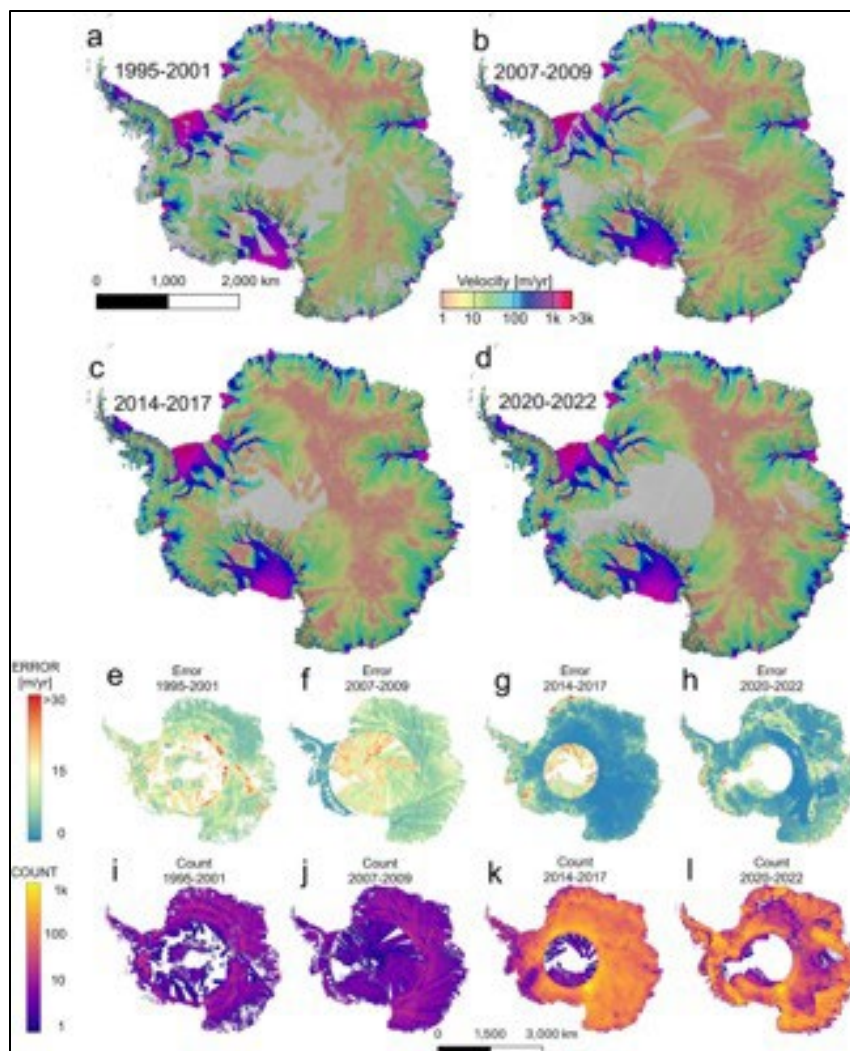


Figure 1. Ice motion from (a) 1995–2001; (b) 2007–2009; (c) 2014–2017; and (d) 2020–2022, color coded on a log scale from brown (low velocity) to yellow, green, blue and purple (high velocity), plus error in speed (e–h) and pair count (i–l) for each of the mosaics. (Rignot, et al., 2022)

3 VERSION HISTORY

| Version | Release Date | Description of Changes |
|---------|--------------|---|
| V1.1 | Apr. 2026 | <ul style="list-style-type: none"> Temporal coverage extended with map for 1 July 2020 – 30 June 2022 Previously published V1.0 files reprocessed to correct file metadata error that specified “06-31” (i.e., June 31) in “time_coverage_end” attribute. |
| V1.0 | Oct. 2022 | Initial release |

4 RELATED DATA SETS

- [MEaSURES InSAR-Based Antarctica Ice Velocity Map](#)
- [MEaSURES Phase-Based Antarctica Ice Velocity Map](#)
- [MEaSURES Annual Antarctic Ice Velocity Maps](#)
- [MEaSURES Antarctic Grounding Line from Differential Satellite Radar Interferometry](#)
- [MEaSURES BedMachine Antarctica](#)
- [MEaSURES InSAR-Based Ice Velocity of the Amundsen Sea Embayment, Antarctica](#)
- [MEaSURES Antarctic Boundaries for IPY 2007-2009 from Satellite Radar](#)

5 RELATED WEBSITES

[MEaSURES Data | Overview](#)

6 ACKNOWLEDGMENTS

This data set was generated through a grant from the NASA MEaSURES program.

RADARSAT-1 data were acquired as part of the Antarctic Mapping Mission (AMM) in 1997 and the Modified Antarctic Mapping Mission (MAMM) in late 2000. ERS-1/2 acquired data in coastal Antarctica in 1996. Data acquisitions between 2006 and 2016 are courtesy of the International Polar Year (IPY) Space Task Group and its successor, the Polar Space Task Group (PSTG).

In addition, this data set utilizes modified Copernicus Sentinel-1 data (2014-2016), acquired by the ESA, distributed through the Alaska Satellite Facility, and processed by Rignot, E, J. Mouginot, and B. Scheuchl.

The TanDEM-X DEM of Antarctica was provided by the DLR.

7 REFERENCES

Li, X., Rignot, E., Mouginot, J., & Scheuchl, B. (2016). Ice flow dynamics and mass loss of Totten Glacier, East Antarctica, from 1989 to 2015. *Geophysical Research Letters*, *43*(12), 6366–6373. doi: [10.1002/2016GL069173](https://doi.org/10.1002/2016GL069173).

Michel, R., & Rignot, E. (1999). Flow of Glacier Moreno, Argentina, from repeat-pass Shuttle Imaging Radar images: Comparison of the phase correlation method with radar interferometry. *Journal of Glaciology*, *45*(149), 93–100. doi: [10.3189/S0022143000003075](https://doi.org/10.3189/S0022143000003075).

Mouginot, J., Rignot, E., & Scheuchl, B. (2014). Sustained increase in ice discharge from the Amundsen Sea Embayment, West Antarctica, from 1973 to 2013. *Geophysical Research Letters*, *41*(5), 1576–1584. doi: [10.1002/2013GL059069](https://doi.org/10.1002/2013GL059069).

Mouginot, J., Rignot, E., & Scheuchl, B. (2019). Continent-Wide, Interferometric SAR Phase, Mapping of Antarctic Ice Velocity. *Geophysical Research Letters*, *46*(16), 9710–9718. doi: [10.1029/2019GL083826](https://doi.org/10.1029/2019GL083826).

Mouginot, J., Rignot, E., Scheuchl, B., & Millan, R. (2017). Comprehensive annual ice sheet velocity mapping using Landsat-8, Sentinel-1, and RADARSAT-2 data. *Remote Sensing*, *9*(4), 364. doi: [10.3390/rs9040364](https://doi.org/10.3390/rs9040364).

Mouginot, J., Scheuchl, B., & Rignot, E. (2012). Mapping of ice motion in Antarctica using Synthetic-Aperture Radar data. *Remote Sensing*, *4*(9), 2753–2767. doi: [10.3390/rs4092753](https://doi.org/10.3390/rs4092753).

Rignot, E., Mouginot, J., Scheuchl, B., & Jeong, S. (2022). Changes in Antarctic Ice Sheet Motion Derived From Satellite Radar Interferometry Between 1995 and 2022. *Geophysical Research Letters*, *49*(23). <https://doi.org/10.1029/2022gl100141>

Rignot, E., Mouginot, J., Scheuchl, B., van den Broeke, M., van Wessem, M. J., & Morlighem, M. (2019). Four decades of Antarctic ice sheet mass balance from 1979–2017. *Proceedings of the National Academy of Sciences*, *116*(4), 1095–1103. doi: [10.1073/pnas.1812883116](https://doi.org/10.1073/pnas.1812883116).

Rignot, E., Jacobs, S., Mouginot, J., & Scheuchl, B. (2013). Ice-shelf melting around Antarctica. *Science*, *341*(6143), 266–270. doi: [10.1126/science.1235798](https://doi.org/10.1126/science.1235798).

Rignot, E., Mouginot, J., & Scheuchl, B. (2011a). Antarctic grounding line mapping from differential satellite radar interferometry: *Geophysical Research Letters*, *38*(10). doi: [10.1029/2011GL047109](https://doi.org/10.1029/2011GL047109).

Rignot, E., Mouginot, J., & Scheuchl, B. (2011b). Ice flow of the Antarctic ice sheet. *Science*, *333*(6048), 1427–1430. doi: [10.1126/science.1208336](https://doi.org/10.1126/science.1208336).

Rignot, E., Bamber, J. L., van den Broeke, M. R., Davis, C., Li, Y., van de Berg, W. J., & van Meijgaard, E. (2008). Recent Antarctic ice mass loss from radar interferometry and regional climate modelling. *Nature Geoscience*, 1(2), 106–110. doi: [10.1038/ngeo102](https://doi.org/10.1038/ngeo102).

Scheuchl, B., Mouginot, J., & Rignot, E. (2012). Ice velocity changes in the Ross and Ronne sectors observed using satellite radar data from 1997 and 2009. *The Cryosphere*, 6(5), 1019–1030. doi: [10.5194/tc-6-1019-2012](https://doi.org/10.5194/tc-6-1019-2012).

8 DOCUMENT INFORMATION

8.1 Publication Date

October 2022

8.2 Date Last Updated

April 2026

APPENDIX A – SPATIAL AND TEMPORAL COVERAGE BY SATELLITE

Table A - 1: Satellite Data Temporal and Spatial Coverage

| Platform/Sensor | Agency | Look Dir. | Mode | Repeat Cycle (day) | Incidence Angle | Resolution Rg x Az (m) | Freq (GHz) | Year |
|-------------------------|-------------------|------------|--------------|--------------------|-----------------|------------------------|------------|-------------------------|
| ERS-1 & 2/SAR | ESA ³ | Right | N/A | 1-3 | 23 | 13x4 | 5.33 | 1996 |
| RADARSAT-1/SAR | CSA ⁴ | Left/Right | Varies | 24 | 18-47 | 12x5-17x6 | 5.33 | 1997/2000 |
| ENVISAT/ASAR | ESA | Right | IS2 | 35 | 23 | 13x5 | 5.33 | 2007-2009 |
| RADARSAT-2/SAR | CSA | Left | S5/EH4 | 24 | 41/57 | 12x5 | 5.33 | 2009-2017, 2020-2022 |
| ALOS/PALSAR | JAXA ⁵ | Right | FBS | 46 | 39 | 7x4 | 1.27 | 2006-2010 |
| ALOS-2/PALSAR-2 | JAXA | Left/Right | Varies | 14 | 8-70 | 1x3 | 1.26 | 2014-2017, 2020-2022 |
| Sentinel-1/SAR | ESA | Right | IW-T OPS | 12 | | 12x43 | 5.33 | 2014-2017, 2020-2022 |
| Landsat-8/OLI | USGS/NASA | N/A | Panchromatic | 16 | N/A | 15x15 | | 2013-2017, 2020-2022 |
| TanDEM-X/TerraSAR-X/SAR | DLR ⁶ | Right | N/A | 11 | 46.3 | 1.4x1.8 | 9.65 | 2011-2017 |

³ European Space Agency

⁴ Canadian Space Agency

⁵ Japan Aerospace Exploration Agency

⁶ German Space Agency